

Nanoencapsulation Enhances Epigallocatechin-3-gallate Stability and Its Antiatherogenic Bioactivities in Macrophages

Jia Zhang,^{||} Shufang Nie,^{||} and Shu Wang^{*}

Nutritional Science Program, Texas Tech University, Lubbock, Texas 79409, United States

ABSTRACT: We have successfully synthesized (–)-epigallocatechin-3-gallate (EGCG) encapsulated nanostructured lipid carriers (NLCE) and chitosan-coated NLCE (CSNLCE) using natural lipids, surfactant, chitosan, and EGCG. Nanoencapsulation dramatically improved EGCG stability. CSNLCE significantly increased EGCG content in THP-1-derived macrophages compared with nonencapsulated EGCG. As compared to 10 μ M nonencapsulated EGCG, both NLCE and CSNLCE at the same concentration significantly decreased macrophage cholesteryl ester content. NLCE and CSNLCE significantly decreased mRNA levels and protein secretion of monocyte chemoattractant protein-1 (MCP-1) levels in macrophages, respectively. These data suggest that nanoencapsulated EGCG may have a potential to inhibit atherosclerotic lesion development through decreasing macrophage cholesterol content and MCP-1 expression.

KEYWORDS: EGCG, nanostructured lipid carriers, atherosclerosis, macrophage, stability, uptake

■ INTRODUCTION

Green tea is made from the dried leaves of the *Camellia sinensis* plant and has been considered a healthy beverage since ancient times. Different from fermented black tea and partially fermented oolong tea, green tea is produced from direct drying of fresh green tea leaves by hot steam and air. During this process, polyphenol oxidase is inactivated and catechins are preserved.¹ Green tea contains more catechins than black or oolong tea.² Catechins constitute about 14–33% of the dry green tea leaf weight.^{1,3} (–)-Epigallocatechin-3-gallate (EGCG) is the most abundant green tea catechin and comprises 25–55% of the total catechins.^{1,3} Over the past few decades many scientific and medical studies have already demonstrated many health benefits of green tea including antiatherogenic, anti-inflammatory, and antitumorigenic properties.⁴

Cardiovascular disease (CVD) refers to the class of diseases that involve the heart and blood vessels. CVD is the leading cause of death in the United States and worldwide.^{5,6} About half of the CVD deaths are caused by atherosclerosis, which is a progressive disease characterized by lipid plaque formation in arteries, resulting in insufficient blood supply to heart muscle, brain, or peripheral tissues (for example, legs). Increased lipid accumulation and inflammatory responses are the major causes of atherosclerosis.^{7,8} Monocyte chemoattractant protein 1 (MCP-1) promotes the recruitment of monocytes into the aortic intima layer.⁷ Upon the migration, monocytes are differentiated into macrophages in response to macrophage colony-stimulating factor. These macrophages express scavenger receptors, which increase the uptake of minimally modified low-density lipoprotein (LDL), especially minimally oxidized LDL (oxLDL).⁹ After macrophages accumulate cholesterol, they are transformed into foam cells. Foam cells can secrete many inflammatory factors including MCP-1, which further recruit more monocytes, resulting in increased numbers of macrophages and later foam cells in the artery wall. After foam cells die, lipids (primarily cholesterol) are accumulated on the artery wall and atherosclerotic plaque is formed. Total

cholesterol (TC) in macrophages includes cholesteryl ester (CE), a storage form of cholesterol, and free cholesterol (FC), which can be transported out of macrophages via a process termed reverse cholesterol transport. Foam cell formation and cholesterol accumulation in the vessel intima characterize the atherosclerotic lesion.⁹ Therefore, macrophages play an important role in atherosclerotic lesion progression by facilitating cholesterol accumulation and increasing inflammatory responses in aortic walls.

EGCG has a potential to decrease the release of inflammatory factors and reduce cholesterol accumulation in macrophages,^{10–13} which may in turn prevent atherosclerotic lesion development. When apolipoprotein E null mice are treated with daily intraperitoneal injections of EGCG at a dose of 10 mg/kg body weight, cuff-induced evolving atherosclerotic lesion size is reduced by 55% after 21 days of treatment.¹⁴ Human studies indicate that EGCG can maintain cardiovascular health, but the evidence is inconclusive regarding the effectiveness for CVD prevention or treatment.^{15,16} The major problems are its low stability and bioavailability in humans or research animals.^{17–19} The oral bioavailability of EGCG after drinking tea containing catechins at 10 mg/kg body weight is about 0.1% in humans and research animals.^{18,20} The peak plasma EGCG concentration is 0.15 μ M after consumption of 2 cups of green tea.¹⁹ Moreover, EGCG is unstable in water and physiological fluid *in vitro*.²¹ EGCG stability is lowered by various metabolic transformations including methylation, glucuronidation, sulfation, and oxidative degradation.^{22,23} Hence, there is a critical need to use biocompatible and biodegradable carriers to increase EGCG stability and uptake.

Nanotechnology involves the control of matter, generally in the range of 100 nm or smaller.²⁴ Nanocarriers may increase

Received: May 31, 2013

Revised: August 21, 2013

Accepted: August 26, 2013

Published: August 26, 2013

bioavailability of encapsulated EGCG, enhance its stability, lower its toxicity through preventing EGCG from prematurely interacting with the biological environment, and improve intracellular penetration. Even though nanoparticles have many beneficial effects, they also have many disadvantages including expensive cost, complex synthesis procedures, and potential side effects. We successfully produced biocompatible and biodegradable EGCG encapsulated nanostructured lipid carriers (NLCE), which are composed of natural lipids, surfactant, EGCG, and water. Nanostructured lipid carriers (NLCs) have received considerable attention because of their small size, stability, biocompatibility and biodegradability, low cytotoxicity, and easily scaled-up synthesis processes.²⁵ The NLC structure is composed of a hydrophilic shell and a hydrophobic lipid core, which is solid at room temperature. Chitosan, a natural polysaccharide, is an absorption enhancer.^{26,27} We have synthesized chitosan-coated NLCE (CSNLCE). Our hypothesis is that NLCs and CSNLCEs can increase EGCG stability, increase EGCG uptake by THP-1-derived macrophages, decrease cellular CE content, and lower expression and secretion of inflammatory factors in those macrophages.

MATERIALS AND METHODS

Safety Information. The MTT dye reagent is hazardous; avoid contact with skin and eyes. MTT solvent is flammable and corrosive. Wear lab coat, gloves, and safety glasses when working with this reagent.

Chemicals and Reagents. EGCG (>95%), glyceryl tridecanoate, glyceryl tripalmitate, chitosan with medium molecular weight of 190,000–310,000, phorbol 12-myristate 13-acetate (PMA), and *Escherichia coli* lipopolysaccharide were purchased from Sigma-Aldrich Chemical Co. (St. Louis, MO, USA). Kolliphor HS15 was given as gift from BASF Chemical Co., USA (Florham Park, NJ, USA). Soy lecithin (>95%) and 7-nitro-2-1,3-benzoxadiazol-4-yl-phosphatidylcholine (NBD-PC) were purchased from Avanti Polar Lipids (Alabaster, AL, USA). Trizol reagent, SuperScript III reverse transcriptase, and Power SYBR Green Master Mix were purchased from Life Technologies Co. (Carlsbad, CA, USA).

Preparation of NLCE and CSNLCE. NLC was prepared from a lipid mixture composed of the following lipids in wt %: 9.3 soy lecithin, 40.0 glyceryl tridecanoate, 6.7 glyceryl tripalmitate, 44.0 Kolliphor HS15 (polyoxyethylated 12-hydroxystearic acid, a nonionic surfactant), and an aqueous mixture containing 2.6% EGCG and 1% NaCl in deionized water. A novel phase inversion-based process was used in preparing NLCE.²⁸ Briefly, oil and aqueous phase were heated to 85 °C and mixed together. Then, the mixture was treated with three temperature cycles from 60 to 85 °C and from 85 to 60 °C at a rate of 4 °C/min and stirred at 375 rpm on a magnetic stirrer. In the last cycle, when the mixture was cooled to 70 °C, cold deionized water (0 °C) was added to the mixture. The volume ratio of cold water to lipid was 35:1 in this study. The fast cooling–dilution process resulted in NLCE formation. Afterward, a slow magnetic stirring was applied to the suspension for 45 min. Void nanostructured lipid carriers (VNLC) were synthesized by using the same method without adding EGCG. All steps in the preparation of VNLC and NLCE were performed under nitrogen to prevent EGCG and lipid degradation. NLCE and VNLC were concentrated and coated with 6 mg/mL chitosan using a magnetic stirrer for 40 min at 4 °C to form CSNLCE and chitosan-coated VNLC (VCSNLCE), respectively. The final concentration of chitosan in CSNLCE and VCSNLCE was 2 mg/mL.

Encapsulation Efficiency and Loading Capacity Determination. The total EGCG concentration (C_{total}) in the nanocarrier solution was measured using a high-performance liquid chromatography (HPLC) system (Waters Co., Milford, MA, USA) with a C18 reverse-phase column (150 mm × 4.6 mm, 5 μm size) and a Waters 2489 UV–visible detector. The mixture of water/acetonitrile/ethyl

acetate/sulfuric acid (86:12:2:0.043, v/v/v/v) was used as a mobile phase with a flow rate of 1 mL/min. The detection wavelength was selected as 254 nm. Free EGCG was separated from nanoencapsulated EGCG using an ultrafiltration method (Millipore Amicon Ultra-15) at 1000g at 4 °C for 20 min and measured by the HPLC system (C_{free}). To calculate the loading capacity, a certain volume of NLCE (V) was dried using a vacuum freeze-drying system (FreeZone 4.5 plus, Labconco, Kansas City, MO, USA). The weight of dried NLCE was expressed as W_{NPS} . Dried NLCE was only used for measuring loading capacity. Nanoparticle suspension was used for the rest of other experiments. The encapsulation efficiency and loading capacity of EGCG in the nanocarriers were calculated according to the following equations, respectively:

$$\text{encapsulation efficiency} = (C_{\text{total}} - C_{\text{free}}) / C_{\text{total}} \times 100\%$$

$$\text{loading capacity} = (C_{\text{total}}V - C_{\text{free}}V) / W_{\text{NPS}} \times 100\%$$

Particle Size, Zeta Potential, and Morphology of Nanocarriers. The mean particle size was measured by dynamic light scattering (DLS); polydispersity index (PI) and zeta potential of nanocarriers were measured using a ZetaPALS analyzer (Brookhaven Corp., Holtsville, NY, USA). The morphology of the NLCE and CSNLCE was examined using a transmission electron microscope (TEM) instrument (200 kV Hitachi H-8100, Tokyo, Japan).

Stability Study of NLCE, CSNLCE, and Nonencapsulated EGCG. The stabilities of NLCE, CSNLCE, and nonencapsulated EGCG were determined in 1× phosphate-buffered saline (1× PBS) at pH 1.0, 3.0, 5.0, and 7.4. Hydrochloric acid was used to adjust the pH. The final concentration of nanoencapsulated and nonencapsulated EGCG was 100 μM. The solutions were stored in tightly closed vials and incubated at 37 °C. EGCG concentrations were measured after incubation for 0, 0.25, 0.5, 0.75, 1.0, 1.5, 2.0, and 3.0 h. To determine the EGCG stability at different temperatures, 100 μM nonencapsulated EGCG and nanoencapsulated EGCG (NLCE and CSNLCE) dissolved in 1× PBS (pH 7.4, ionic strength = 157.5 mM) were incubated at 4 °C for 14 days, at 22 °C for 19 h, and at 37 °C for 3 h. We also measured their stability in RPMI 1640 cell culture medium at 37 °C with or without cells and with or without superoxide dismutases (SOD, 5 U/mL).

In Vitro Release Study. The in vitro release behaviors of nonencapsulated EGCG and NLCE were measured in 1× PBS (pH 5.0) using a dialysis method. Samples of 1.0 mg of nonencapsulated EGCG and an equivalent amount in NLCE were dissolved in 2 mL of 1× PBS (pH 5.0) and then placed in the dialysis bags with MWCO 6000–8000. The dialysis bags were dipped in a conical flask containing 25 mL of 1× PBS (pH 5.0) (dissolution medium) at 37 °C and stirred at 250 rpm. The dissolution medium was totally replaced by fresh prewarmed medium every 2 h to minimize the effect of EGCG degradation. The EGCG released into the medium was determined every 30 min using the HPLC system.

Cytotoxicity Analysis. Human monocytic THP-1 cell line was purchased from the American Type Tissue Culture Collection (ATCC, Manassas, VA, USA) and cultured in the RPMI 1640 medium following ATCC instructions. THP-1 cells (3×10^4 /well) in a 96-well plate were differentiated into macrophages by incubation with 50 ng/mL PMA for 72 h. The THP-1-derived macrophages were treated with 1× PBS, nonencapsulated EGCG, VNLC, NLCE, VCSNLCE, and CSNLCE dissolved in 1× PBS (pH 7.4) for 18 h. Three EGCG concentrations (5, 10, and 20 μM) were tested. The cell viability was measured using a 3-(4,5-dimethylthiazol-2-yl)-2,5-diphenyltetrazolium bromide (MTT) assay as previously described.²⁹ Three independent experiments were conducted with six replicates within one experiment.

Binding and Uptake of Fluorescent Dye-Labeled Nanocarriers. We used the above phase inversion-based process to synthesize NBD-PC-labeled VNLC (NBD-VNLC) by replacing 1.0 mol % of total lipids with NBD-PC and coated them with chitosan to form NBD-PC-labeled VCSNLCE (NBD-VCSNLCE). After incubation of THP-1-derived macrophages with NBD-VNLC or NBD-VCSNLCE, or 1× PBS (pH 7.4) used as control, at 4 and 37 °C, cellular binding

Table 1. Particle Size, Zeta Potential, and Polydispersity Index (PI) of Nanocarriers

temperature (°C)	nanocarrier	particle size (nm)		zeta potential (mV)		PI	
		0 days	50 days	0 days	50 days	0 days	50 days
4	VNLC	43.1 ± 3.3	51.4 ± 0.8	-8.9 ± 3.0	-7.2 ± 1.3	0.28 ± 0.03	0.24 ± 0.03
	NLCE	46.3 ± 1.4	51.8 ± 1.8	-12.6 ± 3.2	-8.8 ± 0.2	0.19 ± 0.01	0.18 ± 0.02
	VCSNLC	48.0 ± 0.7	54.2 ± 0.7	20.9 ± 0.4	15.3 ± 1.8	0.25 ± 0.03	0.25 ± 0.04
	CSNLCE	53.5 ± 1.6	70.6 ± 0.5	13.3 ± 1.0	13.0 ± 4.3	0.19 ± 0.01	0.29 ± 0.01
temperature (°C)	nanocarrier	particle size (nm)		zeta potential (mV)		PI	
		0 h	24 h	0 h	24 h	0 h	24 h
37	VNLC	43.1 ± 3.3	43.9 ± 2.3	-8.9 ± 3.0	-5.2 ± 1.8	0.28 ± 0.03	0.20 ± 0.03
	NLCE	46.3 ± 1.4	47.1 ± 1.9	-12.6 ± 3.2	-8.7 ± 4.5	0.19 ± 0.01	0.19 ± 0.03
	VCSNLC	48.0 ± 0.7	52.7 ± 3.1	20.9 ± 0.4	8.2 ± 4.7	0.25 ± 0.03	0.36 ± 0.02
	CSNLCE	53.5 ± 1.6	56.5 ± 3.2	13.3 ± 1.0	6.9 ± 2.6	0.19 ± 0.01	0.28 ± 0.02

and uptake of NBD-VNLC and NBD-VCSNLC were observed under a fluorescence microscopy (Olympus, USA) as previously described.²⁹ Microscopy settings were identical for all measures to allow equal comparison of the images. Fluorescence intensities were quantified using NIH imageJ software.

Cellular EGCG Content. THP-1-derived macrophages were incubated with 100 μ M nonencapsulated EGCG and nanoencapsulated EGCG (NLCE and CSNLCE) in RPMI 1640 medium with or without SOD (5 U/mL) for 2 and 4 h at 4 or 37 °C. After cells had been washed, the cellular EGCG was extracted and determined as previously described.²⁹ Total cellular protein levels were determined by using a bicinchoninic acid (BCA) kit (Pierce, Rockford, IL, USA). Cellular EGCG content was expressed as micrograms of EGCG per milligram of protein.

Minimally Oxidized LDL Preparation and Cellular Cholesterol Content Measurement. LDL was isolated from human plasma by a sequential ultracentrifugation method.³⁰ Minimally oxidized LDL (oxLDL) was prepared by an adaptation of a previously described method.³⁰ THP-1-derived macrophages of 1.5×10^6 /well in 6-well plates were incubated with or without 40 mg protein/mL of minimally oxLDL in combination with the following treatments: 1 \times PBS, nonencapsulated EGCG, VNLC, NLCE, VCSNLC, and CSNLCE containing 10 μ M EGCG for 18 h. After cellular lipid extraction using a chloroform and methanol mixture (2:1, v/v), FC and TC were measured using a HPLC system as previously described.³⁰ Stigmasterol was used as internal standard. Delipidated cellular protein levels were determined using a BCA kit. CE was calculated as the difference between TC and FC and expressed as micromoles of cholesterol per gram of protein.

Secretion of Inflammatory Factors. THP-1-derived macrophages were pretreated with 10 μ M VNLC, VCSNLC, NLCE, CSNLCE, EGCG, and 1 \times PBS for 2 h. Then, 50 ng/mL *E. coli* lipopolysaccharide (Sigma) was added into each well and incubated for an additional 16 h. Tumor necrosis factor alpha (TNF α), interleukin-6 (IL-6), and MCP-1 protein concentrations in the culture medium were determined using DuoSet ELISA kits (R&D Systems, Minneapolis, MN, USA) as previously described.³⁰

Real-Time Polymerase Chain Reaction. RNA was extracted from THP-1-derived macrophages using a Trizol reagent. cDNA was synthesized from RNA using SuperScript III reverse transcriptase according to the manufacturer's instructions. MCP-1 and TNF α primers were designed and tested in our previous publication.³⁰ β -Actin was used as an endogenous control. cDNA levels of MCP-1 and TNF α were measured using Power Sybr Green Master Mix on a real-time PCR system (Eppendorf, Hauppauge, NY, USA). mRNA-fold change was calculated using the $2(-\Delta\Delta C(T))$ method.³⁰

Statistical Analysis. Data analysis was conducted using Statistical Package for the Social Sciences (SPSS). One-way ANOVA followed by Tukey's HSD post hoc test was performed to compare multiple group means. Independent Student's *t* test was performed to compare two group means. Differences were considered statistically significant at $p < 0.05$. Data in figures and tables are expressed as means \pm standard deviation (SD).

RESULTS AND DISCUSSION

Characteristics of Nanocarriers. EGCG is a promising natural compound for atherosclerosis prevention and treatment. However, its low levels of stability and cellular bioavailability limit its antiatherogenic activity. Two approaches have been used to increase its stability and bioactivities: (i) formation of the peracetate ester of EGCG³¹ or EGCG-docosapentaenoic acid ester;³² (ii) using nanocarriers such as nanoliposomes²⁹ and NLCs.³³ The chemical modification makes lipophilic EGCG prodrugs, which require chemical cleavage before releasing nonencapsulated EGCG. Nanoliposomes per se are not stable, and encapsulated compound can be leaked out. NLCs do not have those problems and have been widely used in pharmaceutical and nutraceutical research. In this study, NLCE and CSNLCE were successfully synthesized using biocompatible and biodegradable triglyceride, phosphatidylcholine, Kolliphor HS15, NaCl, chitosan, and EGCG. The size of VNLC and NLCE was about 45 nm in diameter, and coating them with chitosan increased the size to about 50 nm (Table 1). PI values were relatively low (<0.3), which indicates a high level of uniformity (Table 1). Studies have shown that nanocarriers smaller than 100 nm are cleared much more slowly than large carriers by the reticulo-endothelial system in the liver and spleen.^{24,34} VNLC and NLCE were negatively charged. After they had been coated with chitosan, VCSNLC and CSNLCE became slightly larger and positively charged (Table 1). Chitosan is a natural and biocompatible polysaccharide obtained by deacetylation of chitin from the exoskeleton of crustaceans such as crabs and shrimps, which can enhance the stability and bioavailability of nanocarriers and nanoencapsulated compounds.³⁵

Table 1 also shows the changes of particle size, PI, and zeta potential of NLCE and CSNLCE in deionized water at 4 and 37 °C. After 4 °C storage for 50 days, the size, PI, and zeta potential of VNLC, NLCE, and VCSNLC were slightly changed, but the size and PI of CSNLCE were increased >1.3-fold. Surface charge is important in nanocarrier systems. In general, higher absolute surface charge leads to stronger repulsion interactions among nanocarriers and, hence, higher stability. After incubation at 37 °C for 24 h, the size and PI of nanocarriers did not change dramatically, but the absolute zeta potential values were decreased. In this study, mixing glyceryl tridecanoate and glyceryl tripalmitate can form less perfect crystals in the lipid core, which can accommodate more EGCG. The encapsulation efficiency is about 99% and loading capacity is around 3%. Glyceryl tridecanoate is solid at room temperature and liquid in body temperature, which can

improve EGCG storage stability *in vitro* and bioactivity *in vivo*. Both NLCE and CSNLCE were spherical under TEM (Figure 1). The average size of NLCE and CSNLCE measured using

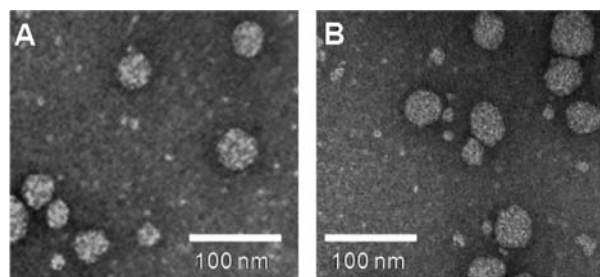


Figure 1. Transmission electron microscope (TEM) image of NLCE (A) and CSNLCE (B) stained by 2% uranyl acetate.

TEM was consistent with the DLS measures. Many studies indicated that the nature and amounts of surfactants and lipids determine the characteristics of nanocarriers, such as particle size and encapsulation efficiency.^{33,36} Higher lipid amounts (larger hydrophobic core) can accommodate more EGCG, but form large nanocarriers.³⁷ The particle size of nanocarriers was dependent on the ratio of lipids to surfactants. Consistent with other studies,^{33,36} we found that as the ratio of triglycerides to Kolliphor HS15 was decreased, the size of nanocarriers was decreased (data not shown). On the basis of these preliminary data, we chose a 1:1 ratio of triglycerides to Kolliphor HS15, which gave small size (48 nm in diameter) and high encapsulation efficiency (about 99%).

Chemical Stability of NLCE, CSNLCE, and Non-encapsulated EGCG. We measured the chemical stability of 100 μM nonencapsulated and nanoencapsulated EGCG in different temperatures and pH values. NLCE, CSNLCE, and nonencapsulated EGCG were stable in the acidic pH ranging from 1.0 to 5.0 at 37 $^{\circ}\text{C}$ for 3 h (data not shown). EGCG is unstable under alkaline or neutral conditions.³⁸ In the neutral pH 7.4, nanoencapsulation significantly increased the percentage of EGCG remaining at three tested temperatures (4, 25, and 37 $^{\circ}\text{C}$) (Figure 2). At 4 $^{\circ}\text{C}$, 100% of nonencapsulated EGCG was degraded after 1 day, whereas the degradation rate of EGCG in NLCE and CSNLCE was <5%. After 14 days, 75 and 25% of EGCG remained in CSNLCE and NLCE at 4 $^{\circ}\text{C}$ (Figure 2A). After 8 h of incubation at 22 $^{\circ}\text{C}$, the percentages of EGCG remaining in nonencapsulated EGCG, NLCE, and CSNLCE were 1.5, 55, and 89%, respectively (Figure 2B). At 37 $^{\circ}\text{C}$, nonencapsulated EGCG were completely degraded after 3 h; however, the percentages of EGCG remaining in NLCE and CSNLCE were 33 and 64%, respectively (Figure 2C). In addition, concentrated nanoencapsulated EGCG can be stored at 4 $^{\circ}\text{C}$ for a long period of time without obvious degradation. After storing NLCE and CSNLCE in neutral 1 \times PBS containing 3000 μM nanoencapsulated EGCG at 4 $^{\circ}\text{C}$ for 50 days, we still detected 82 and 92% of EGCG in NLCE and CSNLCE, respectively. These results indicated that nanoencapsulation significantly increased EGCG stability. NLC has a solid lipid core at room temperature. Amphiphilic and pH-sensitive compounds can be easily encapsulated into the lipid core and are stable in the solid lipid core.³⁹ Recently, many studies indicated that green tea catechins may undergo degradation, oxidation, epimerization, and polymerization, which could be contributed by many factors such as temperature, pH of the system, oxygen levels, and the presence

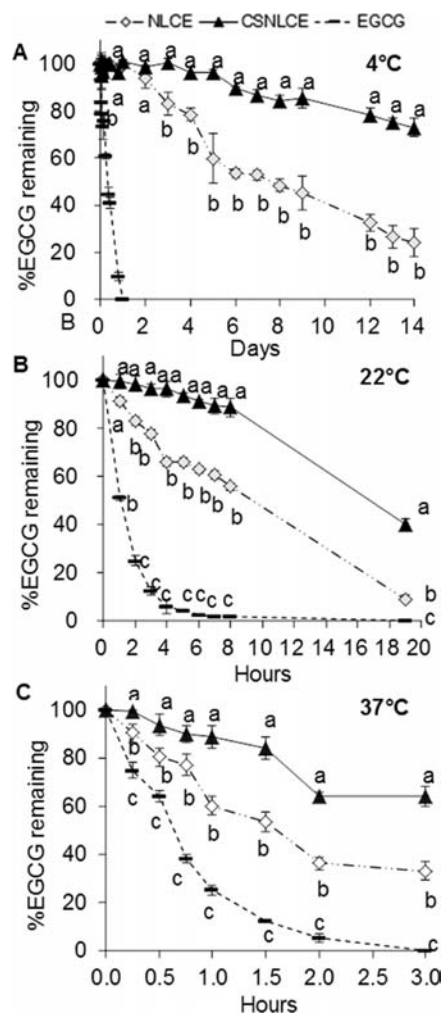


Figure 2. Stability of 100 μM nonencapsulated EGCG, NLCE, and CSNLCE in 1 \times PBS (pH 7.4) at 4 $^{\circ}\text{C}$ (A), 22 $^{\circ}\text{C}$ (B), and 37 $^{\circ}\text{C}$ (C). Means at a time point without a common letter differ, $p < 0.05$.

of metal ions,^{3,40} Nanoencapsulation increases EGCG stability through preventing EGCG from prematurely interacting with the biological environment.^{33,35,41}

Nanoencapsulation also enhances EGCG stability in RPMI 1640 medium at 37 $^{\circ}\text{C}$. After incubation of 100 μM nonencapsulated and nanoencapsulated EGCG in RPMI 1640 medium without THP-1-derived macrophages for 1 h, the percentages of EGCG remaining in nonencapsulated EGCG, NLCE, and CSNLCE were 3.7, 27 and 31%, respectively (Figure 3A). As compared to 1 \times PBS, RPMI 1640 medium decreased the stability of nonencapsulated and nanoencapsulated EGCG (Figures 2C and 3A), which is consistent with EGCG stability order in another study: water > 1 \times PBS > culture medium.⁴² The presence of metal ions and proteins in cell culture might contribute to decreased EGCG stability.²¹ SOD dramatically increased nonencapsulated EGCG stability in RPMI 1640 medium (Figure 3B). Therefore, the stabilities of NLCE, CSNLCE, and nonencapsulated EGCG were similar in the presence of SOD at 37 $^{\circ}\text{C}$ (Figure 3B). In the neutral 1 \times PBS and medium, EGCG is easily autoxidized, forming EGCG dimers. After the addition of SOD into the incubation medium, autoxidation and dimer formation were inhibited.^{21,42}

We measured EGCG concentrations in RPMI 1640 medium in the presence of THP-1-derived macrophages, which were

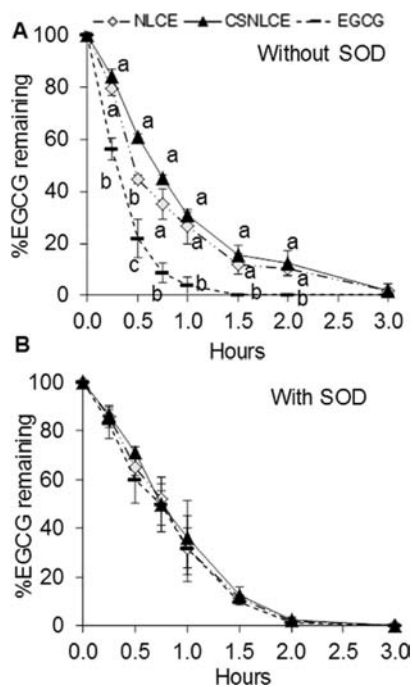


Figure 3. Stability of 100 μM nonencapsulated EGCG, NLCE, and CSNLCE in RPMI 1640 medium at 37 °C in the absence of SOD (A) or in the presence of 5 U/mL SOD (B). Means at a time point without a common letter differ, $p < 0.05$.

treated with 100 μM NLCE, CSNLCE, and nonencapsulated EGCG at 4 and 37 °C. Even though macrophages took up nonencapsulated and nanoencapsulated EGCG from medium, the EGCG concentrations in the medium were higher in the presence of macrophages compared to in the absence of cells at

37 °C (Figures 3 and 4C,D). The concentrations of nanoencapsulated and nonencapsulated EGCG in culture medium were higher at 4 °C compared to 37 °C (Figure 4). SOD increased the concentrations of nanoencapsulated and nonencapsulated EGCG in culture medium at 4 and 37 °C (Figure 4B,D). Hong et al. demonstrated that adding 50 μM EGCG to cell culture medium increased H_2O_2 production, which can decrease EGCG stability.²¹ However, the amount of H_2O_2 was decreased in the presence of cells.²¹ Other studies indicated that increased H_2O_2 production by EGCG instead of direct effects of EGCG resulted in cancer cell growth inhibition and apoptosis in vitro.^{43,44} Cells in the culture medium can produce glutathione peroxidase and catalase, which can decompose H_2O_2 and further improve EGCG stability.^{43,44} On the basis of these data, SOD (5 U/mL) was used to stabilize EGCG for measuring the uptake of nonencapsulated and nanoencapsulated EGCG by macrophages.⁴²

Cellular Binding and Uptake of NBD Nanocarriers.

The binding and uptake of NBD-labeled nanocarriers in THP-1-derived macrophages were observed under a fluorescence microscope after treatment of macrophages with NBD-VNLC (Figure 5A) and NBD-VCSNLC (Figure 5B) for 2, 4, 6, 18, and 24 h at 37 °C and for 4 h at 4 °C. The green and blue colors denote NBD-nanocarriers and cell nuclei, respectively. More NBD-nanocarriers were bound and taken up by macrophages at 37 °C compared to 4 °C. As incubation time was increased, the binding and uptake of NBD-VNLC and NBD-VCSNLC in macrophages were gradually increased and reached the peak at hour 18. After incubation for 24 h, the binding and uptake of NBD-VNLC and NBD-VCSNLC in macrophages were decreased (Figure 5C). Nanocarrier degradation caused by enzymes or environmental factors may partially contribute to the decreased uptake after long-term

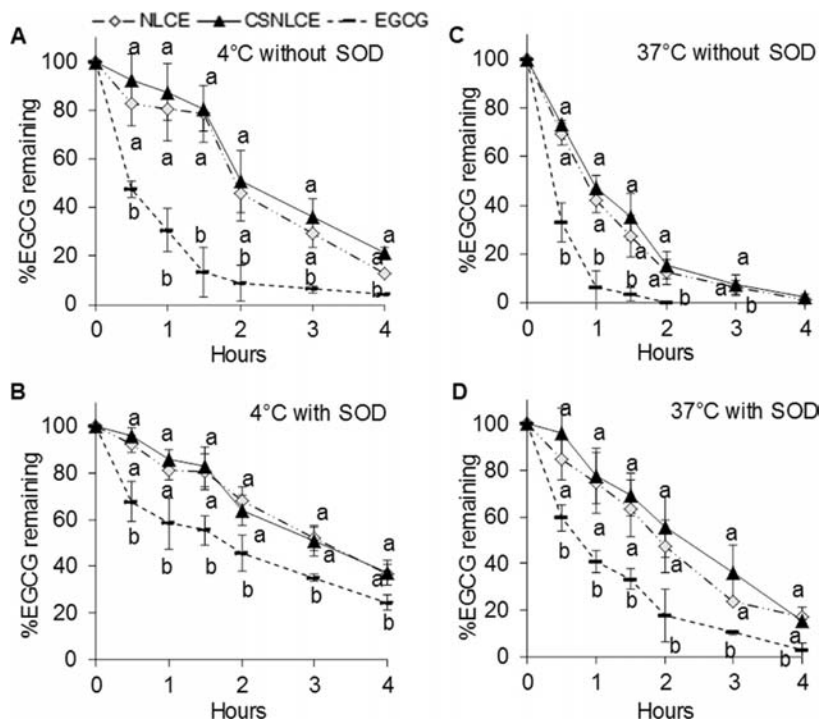


Figure 4. Stability of 100 μM nonencapsulated EGCG, NLCE, and CSNLCE in RPMI 1640 medium in the presence of THP-1-derived macrophages at 4 °C in the absence of SOD (A), at 4 °C in the presence of 5 U/mL of SOD (B), at 37 °C in the absence of SOD (C), or at 37 °C in the presence of 5 U/mL of SOD (D). Means at a time point without a common letter differ, $p < 0.05$.

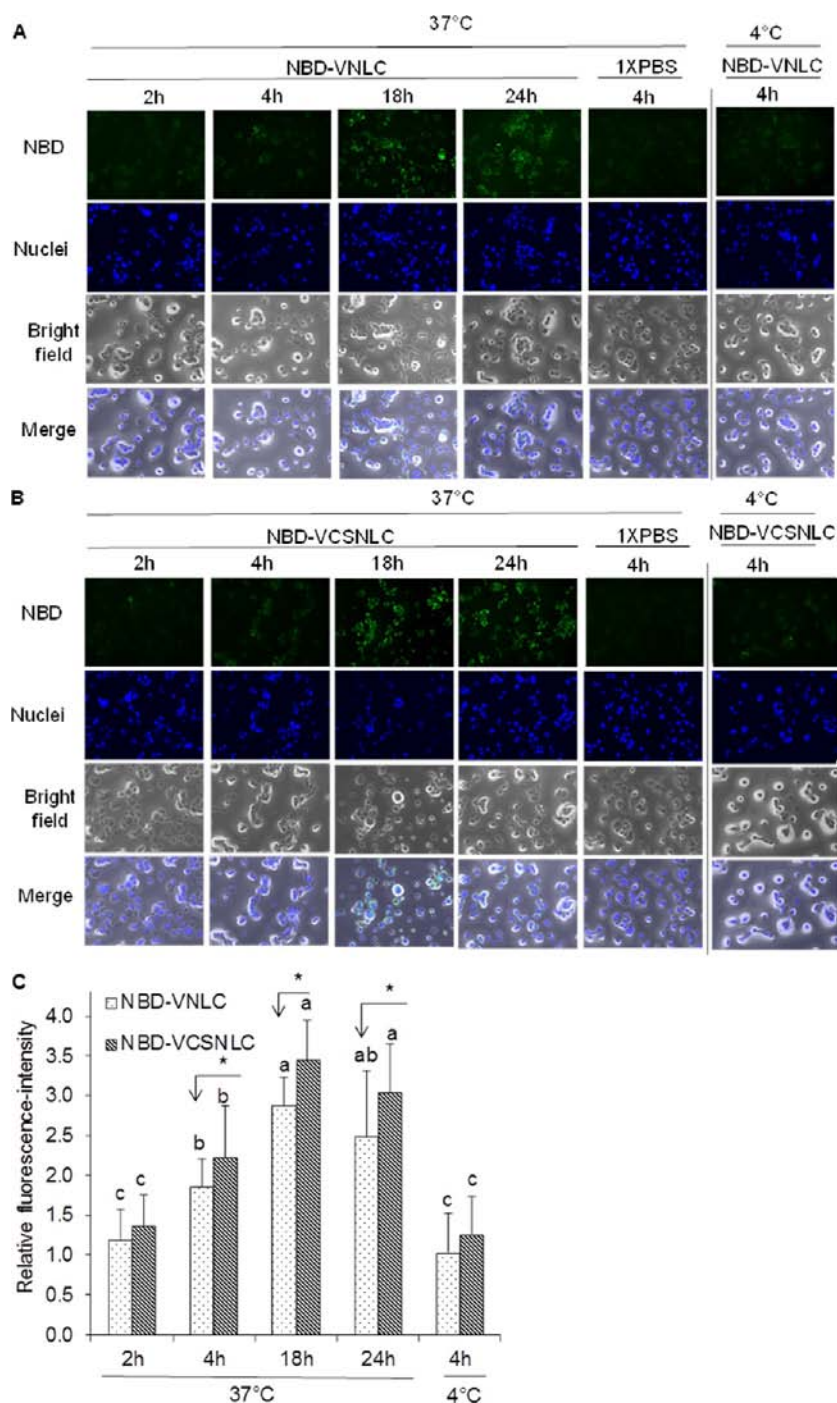


Figure 5. Representative fluorescence images of binding and uptake of NBD-VNLC (A) and NBD-VCSNLC (B) by THP-1-derived macrophages and quantification of relative fluorescence intensities (C). Cells were incubated with NBD-VNLC and NBD-VCSNLC for 2, 4, 18, or 24 h at 37 °C and for 4 h at 4 °C. NBD emitted green fluorescence (λ of excitation is 460 nm, λ of emission is 535 nm); cell nuclei were stained blue by DAPI (λ of excitation is 358 nm, λ of emission is 461 nm). The fluorescence intensity of 1× PBS images was equal to 1. The fluorescence intensities of other images were normalized by the intensity from 1× PBS. Compared to NBD-VNLC, NBD-VCSNLC had higher fluorescence intensities at 37 °C at hours 4, 18, and 24; *, $p < 0.05$; bars without a common letter differ at different incubation time points and temperatures, $p < 0.05$.

incubation. As compared to NBD-VNLC, more NBD-VCSNLC was taken up and bound to macrophages (Figure 5). The data further confirm chitosan is an uptake enhancer. According to fluorescence imaging data, the binding and uptake of NBD-VNLC and NBD-VCSNLC in macrophages were temperature- and time-dependent (Figure 5C).

Macrophage EGCG Content. To measure the cellular EGCG content, THP-1-derived macrophages were incubated

with 100 μM nonencapsulated EGCG, NLCE, and CSNLCE at 4 or 37 °C for 2 and 4 h. After incubation at 37 °C for 2 h in the absence of SOD, the EGCG contents in macrophages treated by nonencapsulated EGCG, NLCE, and CSNLCE were 0.031, 0.096, and 0.14 $\mu\text{g}/\text{mg}$ protein, respectively (data not shown). In the presence of SOD, the EGCG contents were increased to 0.098, 0.176, and 0.307 $\mu\text{g}/\text{mg}$ protein in macrophages treated by nonencapsulated EGCG, NLCE, and

CSNLCE at 37 °C for 2 h, respectively (Figure 6). After incubation at 37 °C for 4 h in the presence of SOD, the EGCG

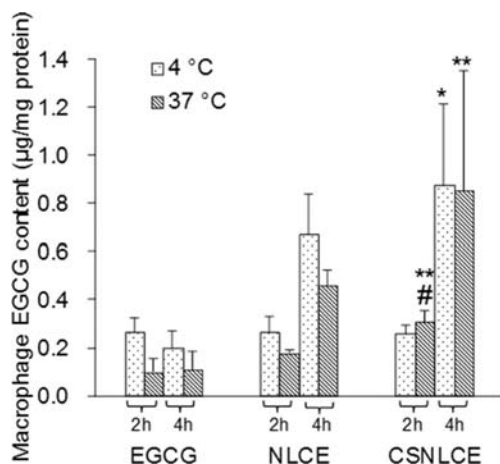


Figure 6. Macrophage EGCG content. THP-1-derived macrophages were treated with 100 μM nonencapsulated EGCG, NLCE, and CSNLCE in RPMI 1640 medium containing SOD (5 U/mL) for 2 and 4 h at 4 or 37 °C. Three independent experiments were conducted. Compared to nonencapsulated EGCG, CSNLCE increased EGCG content; *, $p < 0.05$, and **, $p < 0.01$, compared to NLCE, CSNLCE increased EGCG content; #, $p < 0.05$.

contents in macrophages treated by nonencapsulated EGCG, NLCE, and CSNLCE were 0.109, 0.458, and 0.853 $\mu\text{g}/\text{mg}$ protein, respectively (Figure 6). SOD significantly increased cellular EGCG content among all treatments, which might be partially due to its function in enhancing EGCG stability. No matter in the absence or presence of SOD, nanoencapsulated EGCG, especially CSNLCE, dramatically increased macrophage EGCG content compared to nonencapsulated EGCG (Figure 6). Increased macrophage EGCG content by NLCE and CSNLCE could be partially caused by enhanced EGCG stability. Except nonencapsulated EGCG, 4 h of incubation resulted in higher macrophage EGCG content than 2 h of incubation at both 4 and 37 °C (Figure 6). Consistent with another study,²¹ macrophages incubated with 100 μM nonencapsulated EGCG or NLCE at 4 °C had higher EGCG content than those incubated at 37 °C (Figure 6). The high stability of nonencapsulated EGCG and NLCE at 4 °C may partially contribute to the results. Another reason might be an increase in EGCG efflux from macrophages at 37 °C. Nonencapsulated EGCG at a concentration range from 5 to 640 μM is taken up by cells through a passive diffusion process and subsequently converted to methylated metabolites and glucuronides, which together with nonencapsulated EGCG may be pumped out by cells through multidrug-resistance proteins or P-glycoproteins.^{21,45} This efflux rate was higher at 37 °C than at 4 °C. This energy-dependent efflux process may further explain why cellular EGCG content was higher at 4 °C than at 37 °C.

In Vitro Release Study. The release behavior of nonencapsulated EGCG and NLCE was investigated using a dialysis method. Dynamic dialysis was chosen for separation of free EGCG from NLCE. In Figure 7, nonencapsulated EGCG exhibited a much faster dissolution rate, with 100% released within the initial 2 h period. In contrast, only 2% of EGCG was released from NLCE within the first 2 h. After 9 h, only 4.43% of EGCG was released from NLCE (Figure 7). The data

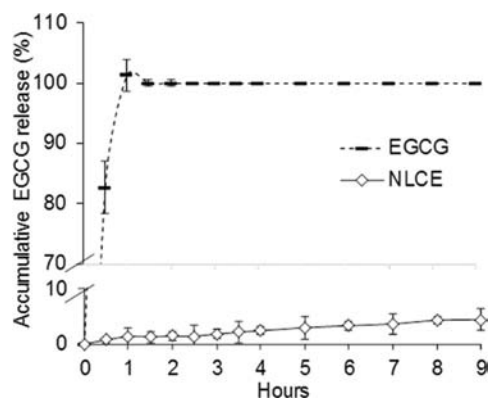


Figure 7. In vitro EGCG release profiles of nonencapsulated EGCG and NLCE. Three independent experiments were conducted.

indicated that increased cellular EGCG content by NLCE was due to uptake of nanocarriers, not nonencapsulated EGCG released from nanocarriers. We confirmed this result with the ultrafiltration method (Millipore Amicon Ultra-15). More studies are required to investigate the membrane receptors in transporting NLCE and CSNLCE, organelles, and enzymes for metabolizing them.

Cytotoxicity Study. After treatment of THP-1 macrophages with 5, 10, and 20 μM nonencapsulated or nanoencapsulated EGCG (NLCE and CSNLCE) and responsive void nanocarriers (VNLC and VCSNLC) for 18 h, the cell viability was >90% among all treatments (Figure 8). The data indicate the NLCE and CSNLCE and their void nanocarriers had a very low level of toxicity in the tested concentration range.

Macrophage Cholesterol Accumulation. In the absence or presence of minimally oxidized LDL in the culture medium, nanoencapsulated EGCG significantly decreased macrophage CE content as compared to 1 \times PBS, nonencapsulated EGCG and void nanocarriers. In the absence of oxLDL, CSNLCE and NLCE resulted in 9.4- and 2.7-fold lower macrophage CE contents than nonencapsulated EGCG, respectively (Figure 9A). In the presence of minimally oxidized LDL, CSNLCE and NLCE resulted in 5.2- and 2.9-fold lower macrophage CE contents than nonencapsulated EGCG, respectively (Figure 9B). Even though NLCE and CSNLCE decreased macrophage TC content, they did not reach a statistical difference due to high standard deviations. The rate-limiting enzyme in cholesterol biosynthesis is 3-hydroxy-3-methylglutaryl-CoA reductase (HMGCR).¹⁰ Nonencapsulated EGCG at 50 μM or higher concentrations can decrease de novo cholesterol synthesis through decreasing HMGCR expression and activity.^{10,46} Miura et al. fed male apolipoprotein E null mice an atherogenic diet (high fat and cholesterol) in combination with a green tea extract drink (0.8 g/L) or a vehicle drink.⁴⁷ The green tea extract drink decreased the atheromatous area and aortic cholesterol content by 23 and 27%, respectively.⁴⁷ In the current study, NLCE and CSNLCE containing 10 μM EGCG significantly decreased macrophage CE content, but nonencapsulated EGCG at the same concentration had no effect on lowering macrophage cholesterol content. The data indicate that nanoencapsulated EGCG retains its bioactivities and exhibits high efficacy at low dose.

Expression and Secretion of Inflammatory Factors. As compared to nonencapsulated EGCG, NLCE significantly decreased mRNA levels of MCP-1 (Figure 10A), and CSNLCE

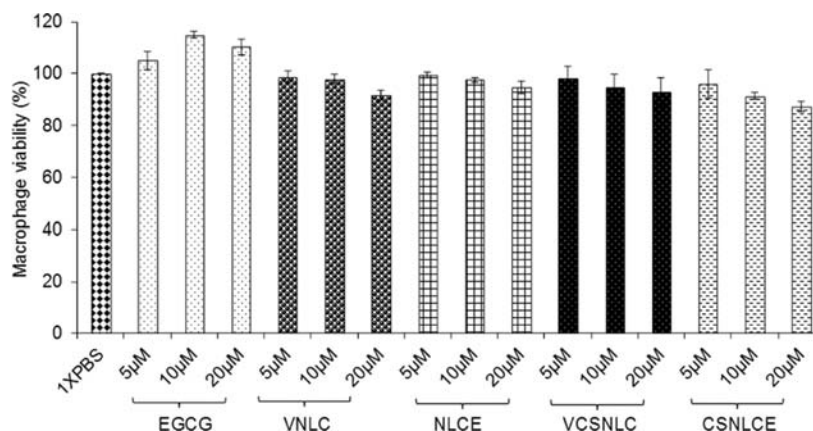


Figure 8. Viability of THP-1-derived macrophages treated by 5, 10, and 20 μM VNLC, VCSNLC, NLCE, CSNLCE, EGCG, and 1 \times PBS for 18 h. Three independent experiments were conducted.

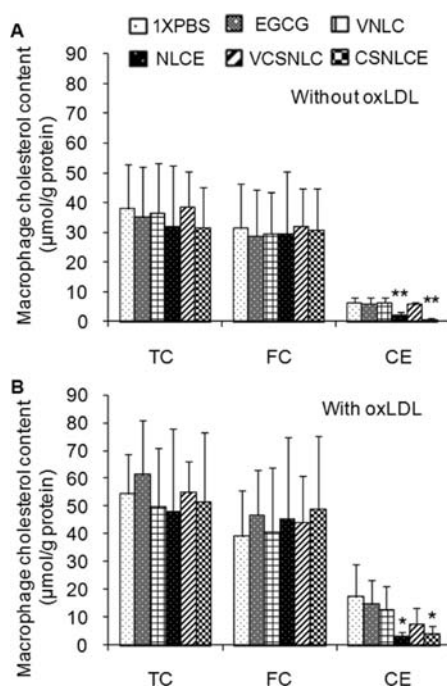


Figure 9. Macrophage cholesterol content. THP-1-derived macrophages were treated with 10 μM VNLC, VCSNLC, NLCE, CSNLCE, EGCG, and 1 \times PBS for 18 h in the absence of minimal oxLDL (A; three independent experiments were conducted) and in the presence of oxLDL (B; six independent experiments were conducted). Compared to 1 \times PBS, EGCG, VNLC, and VCSNLC, NLCE and CSNLCE decreased macrophage CE content; *, $p < 0.05$; **, $p < 0.01$.

significantly decreased MCP-1 release from macrophages (Figure 10B). The release of TNF α and IL-6 from macrophages and mRNA levels of TNF α was similar among all treatments (data not shown). MCP-1 promotes the recruitment of monocytes into the aortic intima layer and atherosclerotic lesion development.⁷ Human studies have shown that elevated plasma MCP-1 concentrations can serve as a direct marker of atherosclerosis.^{7,48} EGCG decreased mRNA and protein levels of MCP-1 in human endothelial cells in a dose-dependent manner (5–30 μM) through inhibiting p38 mitogen-activated protein kinases (MAPK) and nuclear factor-kappaB (NF- κB) activation.¹¹ After treatment of monocytes or macrophages with 100 μM EGCG, MCP-1 expression and secretion and THP-1

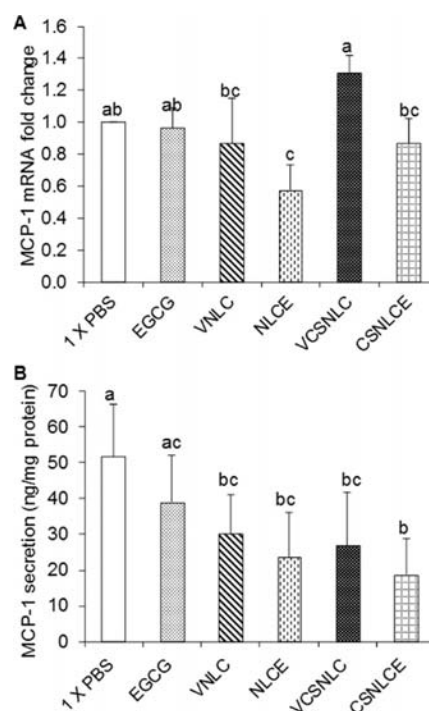


Figure 10. MCP-1 mRNA levels (A) and protein secretion (B) in/ from THP-1-derived macrophages treated with 10 μM VNLC, VCSNLC, NLCE, CSNLCE, EGCG, and 1 \times PBS for 18 h. Three independent experiments were conducted. Bars without a common letter differ, $p < 0.05$.

migration were inhibited via inhibition of NF- κB activation.^{12,13} When rodents were fed a diet containing EGCG, blood MCP-1 concentrations were decreased.^{49,50}

In summary, NLCE and CSNLCE significantly enhanced EGCG stability, improved its sustained release, increased its cellular bioavailability, and decreased cholesterol content and MCP-1 expression in macrophages, which have a potential for preventing and reversing atherosclerotic lesion development.

AUTHOR INFORMATION

Corresponding Author

*(S.W.) Postal address: Nutritional Science Program, Texas Tech University, Box 41240, Lubbock, TX 79409-1240, USA. E-mail: shu.wang@ttu.edu. Phone: (806) 742-3068, ext. 282. Fax: (806) 742-3042.

Author Contributions

J.Z. and S.N. contributed equally to this study and share the first authorship.

Funding

The project described was supported by Grant R15AT007013 from the National Center For Complementary and Alternative Medicine. The content is solely the responsibility of the authors and does not necessarily represent the official views of the National Center For Complementary and Alternative Medicine or the National Institutes of Health.

Notes

The authors declare no competing financial interest.

ACKNOWLEDGMENTS

We thank Ming Sun for giving experimental help.

ABBREVIATIONS USED

EGCG, (–)-epigallocatechin-3-gallate; HPLC, high-performance liquid chromatography; MTT, 3-(4,5-dimethylthiazol-2-yl)-2,5-diphenyltetrazolium bromide; SPSS, Statistical Package for the Social Sciences; ANOVA, one-way analysis of variance; SD, standard deviation; NLCs, nanostructured lipid carriers; NLCE, EGCG-encapsulated nanostructured lipid carriers; CSNLCE, chitosan-coated NLCE; VNLC, void NLC; VCSNLC, void CSNLC; PMA, phorbol 12-myristate 13-acetate; NBD-PC, 7-nitro-2-1,3-benzoxadiazol-4-ylphosphatidylcholine; MCP-1, monocyte chemoattractant protein-1; CVD, cardiovascular disease; LDL, low-density lipoprotein; oxLDL, oxidized LDL; 1× PBS, 1× phosphate-buffered saline; SOD, superoxide dismutase; TEM, transmission electron microscope; FC, nonesterified/free cholesterol; TC, total cholesterol; CE, cholesteryl ester; TNF α , tumor necrosis factor alpha; IL-6, interleukin-6; PI, polydispersity index; HMGCR, 3-hydroxy-3-methylglutaryl-CoA reductase; MAPK, p38 mitogen-activated protein kinases; NF- κ B, nuclear factor-kappaB

REFERENCES

- Wang, S.; Noh, S. K.; Koo, S. I. Green tea catechins inhibit pancreatic phospholipase A(2) and intestinal absorption of lipids in ovariectomized rats. *J. Nutr. Biochem.* **2006**, *17* (7), 492–498.
- Basu, A.; Lucas, E. A. Mechanisms and effects of green tea on cardiovascular health. *Nutr. Rev.* **2007**, *65* (8 Part 1), 361–375.
- Ananingsih, V. K.; Sharma, A.; Zhou, W. B. Green tea catechins during food processing and storage: a review on stability and detection. *Food Res. Int.* **2013**, *50*, 469–479.
- Stangl, V.; Dreger, H.; Stangl, K.; Lorenz, M. Molecular targets of tea polyphenols in the cardiovascular system. *Cardiovasc. Res.* **2007**, *73* (2), 348–358.
- The World Health Organization Report 2007 – Cardiovascular Diseases, 2006.
- Go, A. S.; Mozaffarian, D.; Roger, V. L.; Benjamin, E. J.; Berry, J. D.; Borden, W. B.; Bravata, D. M.; Dai, S.; Ford, E. S.; Fox, C. S.; Franco, S.; Fullerton, H. J.; Gillespie, C.; Hailpern, S. M.; Heit, J. A.; Howard, V. J.; Huffman, M. D.; Kissela, B. M.; Kittner, S. J.; Lackland, D. T.; Lichtman, J. H.; Lisabeth, L. D.; Magid, D.; Marcus, G. M.; Marelli, A.; Matchar, D. B.; McGuiire, D. K.; Mohler, E. R.; Moy, C. S.; Mussolino, M. E.; Nichol, G.; Paynter, N. P.; Schreiner, P. J.; Sorlie, P. D.; Stein, J.; Turan, T. N.; Virani, S. S.; Wong, N. D.; Woo, D.; Turner, M. B. Heart disease and stroke statistics – 2013 update: a report from the American Heart Association. *Circulation* **2013**, *127* (1), e6–e245.
- Martinovic, I.; Abegunewardene, N.; Seul, M.; Vosseler, M.; Horstick, G.; Buerke, M.; Darius, H.; Lindemann, S. Elevated monocyte chemoattractant protein-1 serum levels in patients at risk for coronary artery disease. *Circ. J.* **2005**, *69* (12), 1484–1489.

- Ross, R.; Harker, L. Hyperlipidemia and atherosclerosis. *Science* **1976**, *193* (4258), 1094–1100.

- Guyton, J. R.; Klemp, K. F. Development of the lipid-rich core in human atherosclerosis. *Arterioscler. Thromb. Vasc. Biol.* **1996**, *16* (1), 4–11.

- Cuccioloni, M.; Mozzicafreddo, M.; Spina, M.; Tran, C. N.; Falconi, M.; Eleuteri, A. M.; Angeletti, M. Epigallocatechin-3-gallate potently inhibits the in vitro activity of hydroxy-3-methyl-glutaryl-CoA reductase. *J. Lipid Res.* **2011**, *52* (5), 897–907.

- Hong, M. H.; Kim, M. H.; Chang, H. J.; Kim, N. H.; Shin, B. A.; Ahn, B. W.; Jung, Y. D. (–)-Epigallocatechin-3-gallate inhibits monocyte chemotactic protein-1 expression in endothelial cells via blocking NF- κ B signaling. *Life Sci.* **2007**, *80* (21), 1957–1965.

- Joo, S. Y.; Song, Y. A.; Park, Y. L.; Myung, E.; Chung, C. Y.; Park, K. J.; Cho, S. B.; Lee, W. S.; Kim, H. S.; Rew, J. S.; Kim, N. S.; Joo, Y. E. Epigallocatechin-3-gallate inhibits LPS-induced NF- κ B and MAPK signaling pathways in bone marrow-derived macrophages. *Gut Liver* **2012**, *6* (2), 188–196.

- Melgarejo, E.; Medina, M. A.; Sanchez-Jimenez, F.; Urdiales, J. L. Epigallocatechin gallate reduces human monocyte mobility and adhesion in vitro. *Br. J. Pharmacol.* **2009**, *158* (7), 1705–1712.

- Chyu, K. Y.; Babbidge, S. M.; Zhao, X.; Dandillaya, R.; Rietveld, A. G.; Yano, J.; Dimayuga, P.; Cercek, B.; Shah, P. K. Differential effects of green tea-derived catechin on developing versus established atherosclerosis in apolipoprotein E-null mice. *Circulation* **2004**, *109* (20), 2448–2453.

- Wolfram, S. Effects of green tea and EGCG on cardiovascular and metabolic health. *J Am Coll Nutr* **2007**, *26* (4), 373S–388S.

- Arab, L.; Liu, W.; Elashoff, D. Green and black tea consumption and risk of stroke: a meta-analysis. *Stroke* **2009**, *40* (5), 1786–1792.

- Chen, L.; Lee, M. J.; Li, H.; Yang, C. S. Absorption, distribution, elimination of tea polyphenols in rats. *Drug Metab. Dispos.* **1997**, *25* (9), 1045–1050.

- Warden, B. A.; Smith, L. S.; Beecher, G. R.; Balentine, D. A.; Clevidence, B. A. Catechins are bioavailable in men and women drinking black tea throughout the day. *J. Nutr.* **2001**, *131* (6), 1731–1737.

- Lee, M. J.; Maliakal, P.; Chen, L.; Meng, X.; Bondoc, F. Y.; Prabhu, S.; Lambert, G.; Mohr, S.; Yang, C. S. Pharmacokinetics of tea catechins after ingestion of green tea and (–)-epigallocatechin-3-gallate by humans: formation of different metabolites and individual variability. *Cancer Epidemiol. Biomarkers Prev.* **2002**, *11* (10 Part 1), 1025–1032.

- Lambert, J. D.; Yang, C. S. Mechanisms of cancer prevention by tea constituents. *J. Nutr.* **2003**, *133* (10), 3262S–3267S.

- Hong, J.; Lu, H.; Meng, X.; Ryu, J. H.; Hara, Y.; Yang, C. S. Stability, cellular uptake, biotransformation, and efflux of tea polyphenol (–)-epigallocatechin-3-gallate in HT-29 human colon adenocarcinoma cells. *Cancer Res.* **2002**, *62* (24), 7241–7246.

- Lu, H.; Meng, X.; Yang, C. S. Enzymology of methylation of tea catechins and inhibition of catechol-O-methyltransferase by (–)-epigallocatechin gallate. *Drug Metab. Dispos.* **2003**, *31* (5), 572–579.

- Vaidyanathan, J. B.; Walle, T. Glucuronidation and sulfation of the tea flavonoid (–)-epicatechin by the human and rat enzymes. *Drug Metab. Dispos.* **2002**, *30* (8), 897–903.

- Zhang, L.; Gu, F. X.; Chan, J. M.; Wang, A. Z.; Langer, R. S.; Farokhzad, O. C. Nanoparticles in medicine: therapeutic applications and developments. *Clin. Pharmacol. Ther.* **2008**, *83* (5), 761–769.

- Puri, A.; Loomis, K.; Smith, B.; Lee, J. H.; Yavlovich, A.; Heldman, E.; Blumenthal, R. Lipid-based nanoparticles as pharmaceutical drug carriers: from concepts to clinic. *Crit. Rev. Ther. Drug Carrier Syst.* **2009**, *26* (6), 523–580.

- Dube, A.; Nicolazzo, J. A.; Larson, I. Chitosan nanoparticles enhance the intestinal absorption of the green tea catechins (+)-catechin and (–)-epigallocatechin gallate. *Eur. J. Pharm. Sci.* **2010**, *41* (2), 219–225.

- Dube, A.; Nicolazzo, J. A.; Larson, I. Chitosan nanoparticles enhance the plasma exposure of (–)-epigallocatechin gallate in mice

through an enhancement in intestinal stability. *Eur. J. Pharm. Sci.* **2011**, *44* (3), 422–426.

(28) Heurtault, B.; Saulnier, P.; Pech, B.; Proust, J. E.; Benoit, J. P. A novel phase inversion-based process for the preparation of lipid nanocarriers. *Pharm. Res.* **2002**, *19* (6), 875–880.

(29) de Pace, R. C.; Liu, X.; Sun, M.; Nie, S.; Zhang, J.; Cai, Q.; Gao, W.; Pan, X.; Fan, Z.; Wang, S. Anticancer activities of (–)-epigallocatechin-3-gallate encapsulated nanoliposomes in MCF7 breast cancer cells. *J. Liposome Res.* **2013**, *23* (3), 187–196.

(30) Wang, S.; Wu, D.; Lamon-Fava, S.; Matthan, N. R.; Honda, K. L.; Lichtenstein, A. H. In vitro fatty acid enrichment of macrophages alters inflammatory response and net cholesterol accumulation. *Br. J. Nutr.* **2009**, *102* (4), 497–501.

(31) Lam, W. H.; Kazi, A.; Kuhn, D. J.; Chow, L. M.; Chan, A. S.; Dou, Q. P.; Chan, T. H. A potential prodrug for a green tea polyphenol proteasome inhibitor: evaluation of the peracetate ester of (–)-epigallocatechin gallate [(–)-EGCG]. *Bioorg. Med. Chem.* **2004**, *12* (21), 5587–5593.

(32) Zhong, Y.; Chiou, Y. S.; Pan, M. H.; Shahidi, F. Anti-inflammatory activity of lipophilic epigallocatechin gallate (EGCG) derivatives in LPS-stimulated murine macrophages. *Food Chem.* **2012**, *134* (2), 742–748.

(33) Barras, A.; Mezzetti, A.; Richard, A.; Lazzaroni, S.; Roux, S.; Melnyk, P.; Betbeder, D.; Monfiliette-Dupont, N. Formulation and characterization of polyphenol-loaded lipid nanocapsules. *Int. J. Pharm.* **2009**, *379* (2), 270–277.

(34) Nishiyama, N. Nanomedicine: nanocarriers shape up for long life. *Nat. Nanotechnol.* **2007**, *2* (4), 203–204.

(35) Dube, A.; Nicolazzo, J. A.; Larson, I. Chitosan nanoparticles enhance the intestinal absorption of the green tea catechins (+)-catechin and (–)-epigallocatechin gallate. *Eur. J. Pharm. Sci.* **2010**, *41* (2), 219–225.

(36) Dhawan, S.; Kapil, R.; Singh, B. Formulation development and systematic optimization of solid lipid nanoparticles of quercetin for improved brain delivery. *J. Pharm. Pharmacol.* **2011**, *63* (3), 342–351.

(37) Iqbal, M. A.; Md, S.; Sahni, J. K.; Baboota, S.; Dang, S.; Ali, J. Nanostructured lipid carriers system: recent advances in drug delivery. *J. Drug Target* **2012**, *20* (10), 813–830.

(38) Chen, Z.; Zhu, Q. Y.; Tsang, D.; Huang, Y. Degradation of green tea catechins in tea drinks. *J. Agric. Food Chem.* **2001**, *49* (1), 477–482.

(39) Teeranachaideekul, V.; Muller, R. H.; Junyaprasert, V. B. Encapsulation of ascorbyl palmitate in nanostructured lipid carriers (NLC) – effects of formulation parameters on physicochemical stability. *Int. J. Pharm.* **2007**, *340* (1–2), 198–206.

(40) Wang, R.; Zhou, W.; Jiang, X. Reaction kinetics of degradation and epimerization of epigallocatechin gallate (EGCG) in aqueous system over a wide temperature range. *J. Agric. Food Chem.* **2008**, *56* (8), 2694–2701.

(41) Dube, A.; Nicolazzo, J. A.; Larson, I. Chitosan nanoparticles enhance the plasma exposure of (–)-epigallocatechin gallate in mice through an enhancement in intestinal stability. *Eur. J. Pharm. Sci.* **2011**, *44* (3), 422–426.

(42) Sang, S.; Lee, M. J.; Hou, Z.; Ho, C. T.; Yang, C. S. Stability of tea polyphenol (–)-epigallocatechin-3-gallate and formation of dimers and epimers under common experimental conditions. *J. Agric. Food Chem.* **2005**, *53* (24), 9478–9484.

(43) Long, L. H.; Clement, M. V.; Halliwell, B. Artifacts in cell culture: rapid generation of hydrogen peroxide on addition of (–)-epigallocatechin, (–)-epigallocatechin gallate, (+)-catechin, and quercetin to commonly used cell culture media. *Biochem. Biophys. Res. Commun.* **2000**, *273* (1), 50–53.

(44) Yang, G. Y.; Liao, J.; Li, C.; Chung, J.; Yurkow, E. J.; Ho, C. T.; Yang, C. S. Effect of black and green tea polyphenols on c-jun phosphorylation and H₂O₂ production in transformed and non-transformed human bronchial cell lines: possible mechanisms of cell growth inhibition and apoptosis induction. *Carcinogenesis* **2000**, *21* (11), 2035–2039.

(45) Borst, P.; Evers, R.; Kool, M.; Wijnholds, J. A family of drug transporters: the multidrug resistance-associated proteins. *J. Natl. Cancer Inst.* **2000**, *92* (16), 1295–1302.

(46) Bursill, C. A.; Roach, P. D. Modulation of cholesterol metabolism by the green tea polyphenol (–)-epigallocatechin gallate in cultured human liver (HepG2) cells. *J. Agric. Food Chem.* **2006**, *54* (5), 1621–1626.

(47) Miura, Y.; Chiba, T.; Tomita, I.; Koizumi, H.; Miura, S.; Umegaki, K.; Hara, Y.; Ikeda, M.; Tomita, T. Tea catechins prevent the development of atherosclerosis in apoprotein E-deficient mice. *J. Nutr.* **2001**, *131* (1), 27–32.

(48) Deo, R.; Khera, A.; McGuire, D. K.; Murphy, S. A.; Meo Neto Jde, P.; Morrow, D. A.; de Lemos, J. A. Association among plasma levels of monocyte chemoattractant protein-1, traditional cardiovascular risk factors, and subclinical atherosclerosis. *J. Am. Coll. Cardiol.* **2004**, *44* (9), 1812–1818.

(49) Bose, M.; Lambert, J. D.; Ju, J.; Reuhl, K. R.; Shapses, S. A.; Yang, C. S. The major green tea polyphenol, (–)-epigallocatechin-3-gallate, inhibits obesity, metabolic syndrome, and fatty liver disease in high-fat-fed mice. *J. Nutr.* **2008**, *138* (9), 1677–1683.

(50) Senthil Kumaran, V.; Arulmathi, K.; Sundarapandiyam, R.; Kalaiselvi, P. Attenuation of the inflammatory changes and lipid anomalies by epigallocatechin-3-gallate in hypercholesterolemic diet fed aged rats. *Exp. Gerontol.* **2009**, *44* (12), 745–751.